Table 3.4. *Results for the cube with a linear potential in the x direction*

Model		Charge density at (0.5, 0, 0)					
		Conventional BEM			Fast multipole BEM		
Elem/edge	DOFs	CBIE	HBIE	CHBIE	CBIE	HBIE	CHBIE
2	48	1.08953	1.07225	1.06800	1.08955	1.07278	1.06843
4	192	0.99124	1.00624	0.99754	0.99124	1.00624	0.99754
8	768	0.99825	1.00438	0.99894	0.99825	1.00438	0.99894
12	1728	0.99908	1.00327	0.99934	0.99908	1.00327	0.99934
16	3072	0.99942	1.00260	0.99953	0.99943	1.00260	0.99953
20	4800	0.99959	1.00216	0.99963	0.99962	1.00218	0.99965
24	6912	0.99969	1.00185	0.99970	0.99969	1.00184	0.99969
28	9408	–	–	–	0.99976	1.00161	0.99975
32	12288				0.99981	1.00143	0.99979
Exact value		1.00000					

3.5.3 Potential Field in a Cube

The cube problem used in Subsection 2.12.3 and shown in Figure 2.15 is solved with the 3D fast multipole BEM code and compared with the conventional BEM. For the fast multipole BEM, 15 terms are used in all of the expansions and the tolerance for convergence is set to 10^{-6}.

Table 3.4 shows the results obtained with the fast multipole BEM and compared with those of the conventional BEM, using the CBIE, HBIE, and CHBIE, for BEM meshes with increasing numbers of elements. We can conclude from these results that the HBIE and CHBIE are equally as accurate as the CBIE; so is the fast multipole BEM compared with the conventional BEM. Constant triangular elements are used in this study. If linear or quadratic elements were applied, a few elements should have been sufficient for obtaining results of a similar accuracy because of the specified linear field.

3.5.4 Electrostatic Field Outside Multiple Conducting Spheres

In this example, 11 perfectly conducting spheres (Figure 3.16) are analyzed with the fast multipole BEM. The center large sphere has a radius of 3; the 10 small spheres have the same radius of 1, and are distributed evenly on a circle with a radius of 5 and cocentered with the large sphere. A constant electric potential $\phi = +5$ is applied to the large sphere and five of the small spheres, and a potential $\phi = -5$ is applied to the other five small spheres (Figure 3.16). For the fast multipole BEM, elements per leaf are limited to 200, 10 terms are used in the expansions, and the tolerance for convergence is set to 10^{-4}.

The charge densities on the surfaces of the spheres are plotted in Figure 3.17 with the mesh using 10,800 elements per sphere. The plots are almost

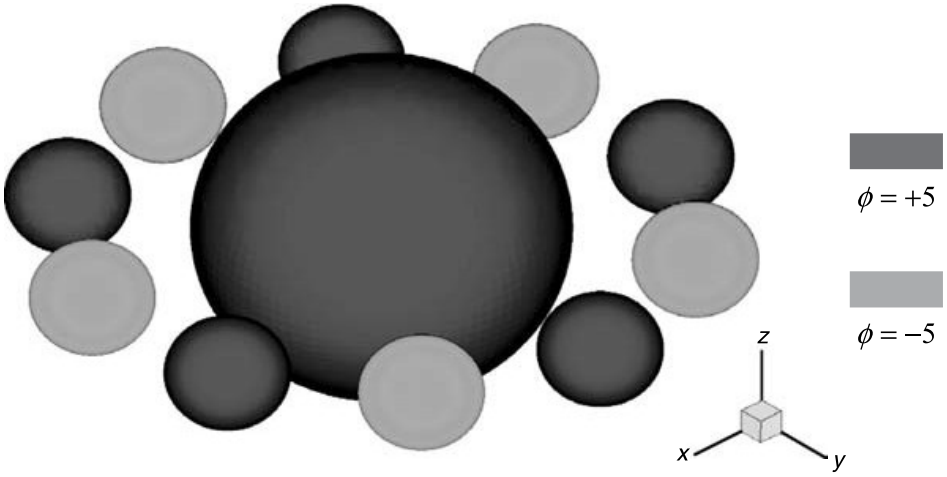

Figure 3.16. An 11-spherical perfect conductor model.

identical among the different meshes and exhibit the same symmetrical pattern, as it should be. Table 3.5 shows the maximum and minimum values of the charge densities on the spheres when the different meshes are used. These values are very stable and converged within the first two significant digits (except for the last set of data with the CBIE). Further improvements can be achieved by using a tighter set of parameters for the fast multipole BEM (e.g., more expansion terms and smaller tolerance). The last two columns of Table 3.5 show the numbers of iterations with the GMRES solver for the CBIE and the CHBIE. The numbers of iterations for the CHBIE is about half those for the CBIE because of the better conditioning of the systems of equations based on the CHBIE.

3.5.5 A Fuel Cell Model

Next, an example of more challenging problems is presented. Figure 3.18(a) shows a solid oxide fuel cell (SOFC) model with nine cells used for thermal analysis. There are 1000 small holes on the inner and outer surfaces of each

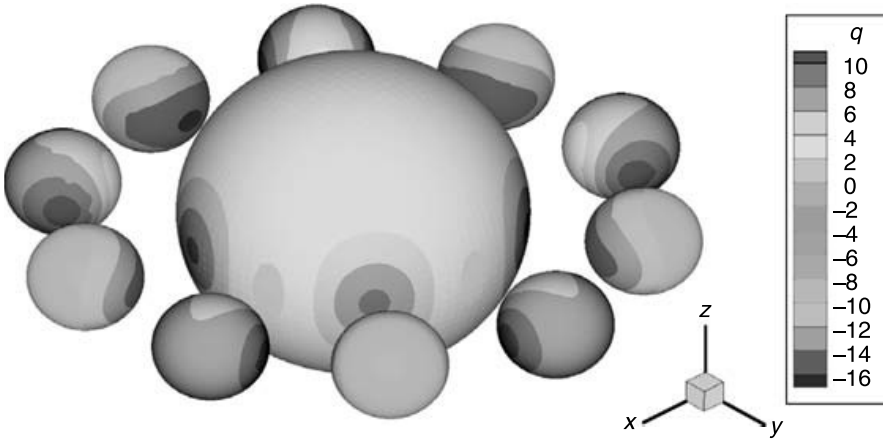

Figure 3.17. Contour plot of the charge densities on the spheres.

Table 3.5. *Results for the 11-sphere model obtained with the fast multipole BEM*

Model		Charge densities on the spheres				Numbers of iterations	
		min		max			
Elem/sphere	DOFs	CBIE	CHBIE	CBIE	CHBIE	CBIE	CHBIE
768	8448	−16.4905	−15.5285	11.1837	10.3923	14	8
1200	13200	−16.5363	−15.7922	11.2218	10.5920	15	8
1728	19008	−16.6322	−15.9618	11.2558	10.7156	17	8
2352	25872	−16.6436	−16.0789	11.2746	10.8041	18	8
3072	33792	−16.6733	−16.1618	11.3792	10.9160	19	8
3888	42768	−16.6648	−16.2195	11.3810	10.9464	20	7
4800	52800	−16.7435	−16.2671	11.3787	10.9763	20	8
7500	82500	−16.7068	−16.3614	11.2964	11.0283	21	8
10800	118800	−17.1157	−16.4279	12.6511	11.0851	22	7

cylindrical cell, with a total of 9000 holes for the entire stack model. Because of the extremely complicated geometry, the FEM (e.g., ANSYS®) can model only one cell on a PC with 1-GB RAM. For the fast multipole BEM, however, multicell models can be handled readily, such as the nine-cell stack modeled successfully with 530,230 elements and solved on a desktop PC with 1-GB RAM [Figure 3.18 (b)].

3.5.6 Image-Based Boundary Element Method Models and Analysis

In recent years, digital models using 3D scanning technologies have attracted much attention in many engineering fields, such as reverse engineering and biomedical engineering applications. Computer-scanned images are often

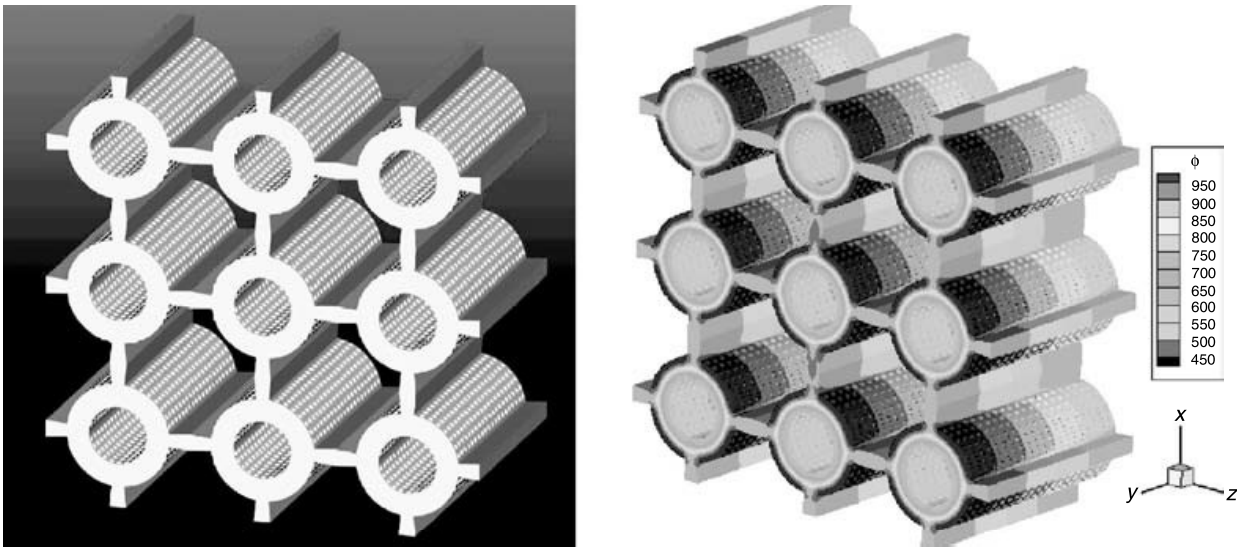

(a) (b)

Figure 3.18. A fuel cell model using the fast multipole BEM: (a) 3 × 3 stack model; (b) computed temperature.